Supporting Information for:

The impact threshold of the aerosol radiation forcing on the boundary layer structure in the pollution region

Dandan Zhao[†1,2]; Jinyuan Xin[*†1,2]; Chongshui Gong[3]; Jiannong Quan[4]; Yuesi Wang[1,2]; Guiqian Tang[1], Yongxiang Ma[1], Lindong Dai[1], Xiaoyan Wu[1], Guangjing Liu[1], Yongjing Ma[1]

1 State Key Laboratory of Atmospheric Boundary Layer Physics and Atmospheric Chemistry (LAPC), Institute of Atmospheric Physics, Chinese Academy of Sciences, Beijing 100029, China

2 University of Chinese Academy of Sciences, Beijing 100049, China

3 Institute of Arid Meteorology, China Meteorological Administration, Lanzhou 730020, China

4 Institute of Urban Meteorology, Chinese Meteorological Administration, Beijing, China

(†) These authors contributed equally to this study.

(*) Correspondence: Jinyuan Xin (xjy@mail.iap.ac.cn;)

The PDF file includes:

Table S1 (Table S1 is referenced in the main manuscript)

Figs. S1 to S4 (Figs. S1 to S5 are referenced in the main manuscript)

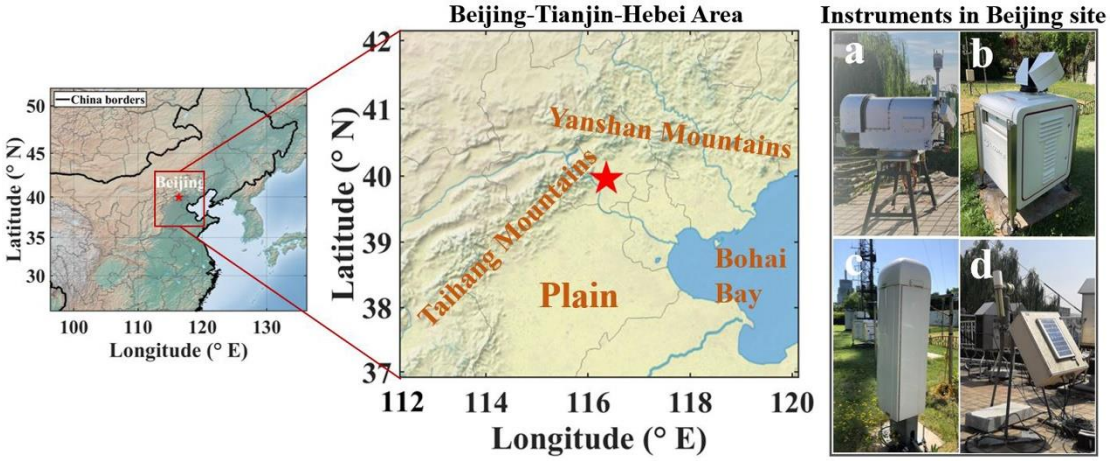

Fig. S1. Left graph is the topographic distribution of most China with Beijing marked by a red star, the middle graph shows the Beijing-Tianjin-Hebei region with the Yanshan Mountains to the north, the Taihang Mountains to the west, and Bohai Bay to the east, and the right graph presents the observation instruments (a: microwave radiometer; b: wind profile lidar; c: ceilometer; d: sun-photometer) used in this study.

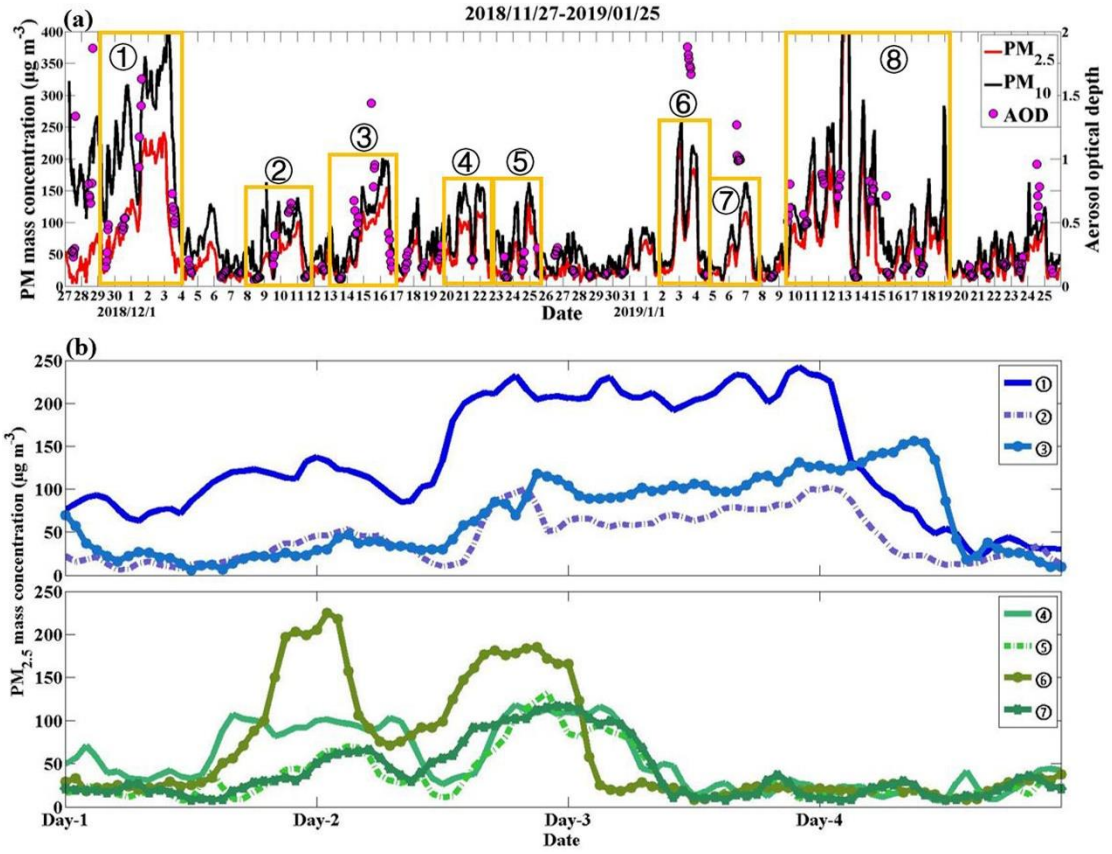

Fig. S2. (a) Temporal evolutions of the PM mass concentration ($PM_{2.5}$: solid red lines; PM_{10}: solid black lines) and aerosol optical depth (AOD; pink circles) from November 27, 2018 to January 25, 2019 in Beijing, with circled boxes represent typical haze pollution episodes named by ①-⑧. (b) Temporal evolutions of the $PM_{2.5}$ mass concentration during typical haze pollution episodes ①-⑦ in Beijing in winter.

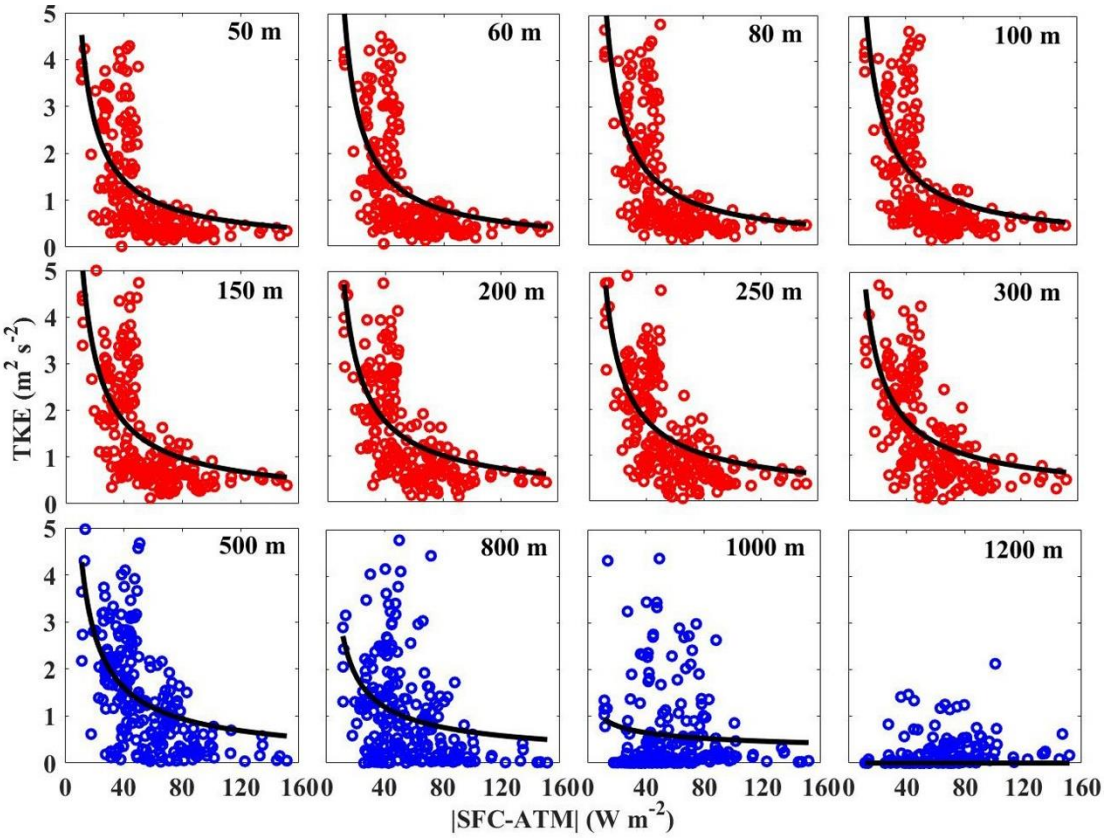

Fig. S3. Scatter plots of the absolute difference of aerosol radiative forcing at the surface and interior of the atmospheric column (|SFC-ATM|; x) versus turbulence kinetic energy (TKE; y) at different altitudes. The calculated hourly data used above were collected over a two-month period in Beijing from 27 November 2018 to 25 January 2019.

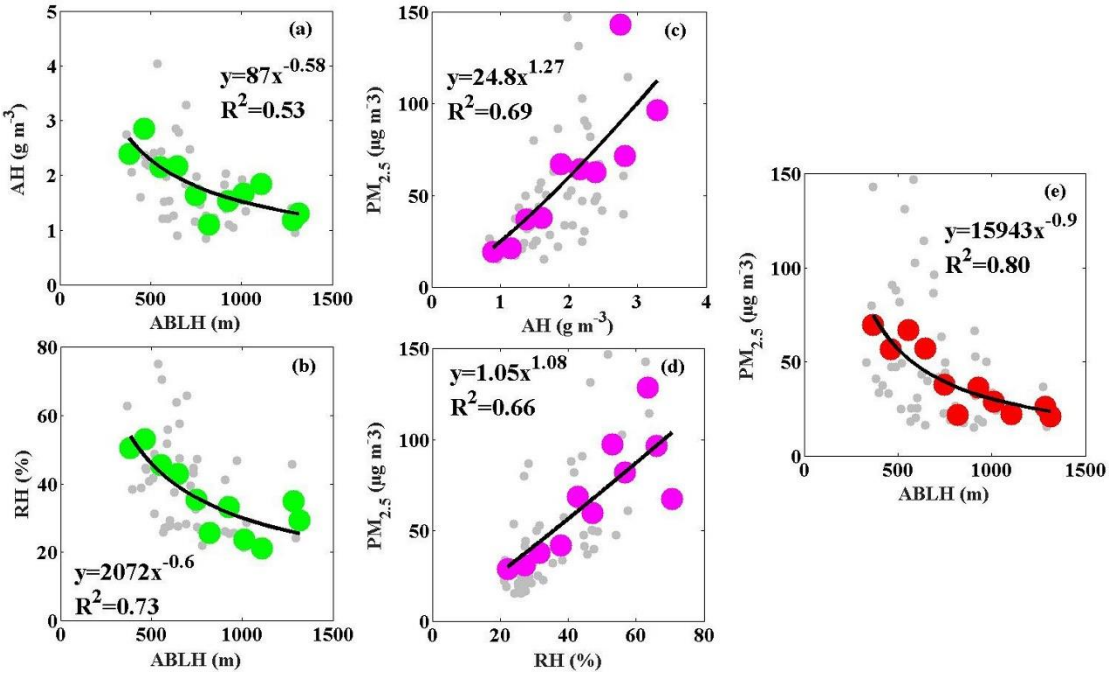

Fig. S4. Scatter plots of the atmospheric boundary layer height (ABLH; x) versus water vapor

density (AH; a) and relative humidity (RH; b), respectively. Scatter plots of water vapor density (AH; c) and relative humidity (RH; d) versus $PM_{2.5}$ concentration, respectively. Scatter plots of ABLH (x) versus $PM_{2.5}$ concentration (e). The calculated daily data used above were over a two-month period in Beijing from 27 November 2018 to 25 January 2019 (gray dots: daily data; other dots: mean data).

Table S1. Equations and correlation coefficients of the fitted curves in Figs. S5 and Figs. 4-5.

	$\|SFC-ATM\|$ vs TKE ($y=ax^b$)			mean $\|SFC-ATM\|$ vs mean TKE ($y=ax^b$)			TKE vs ABLH ($y=ax^b$)		
H (m)	a	b	R^2	a	b	R^2	a	b	R^2
50	43.13	-0.92	0.40	46.90	-0.97	0.91	844.19	0.18	0.13
60	53.77	-0.96	0.40	60.47	-1.02	0.92	827.38	0.19	0.14
80	57.23	-0.96	0.41	66.45	-1.02	0.93	816.67	0.18	0.13
100	51.93	-0.92	0.40	61.69	-0.99	0.93	805.28	0.19	0.14
150	40.46	-0.85	0.41	46.10	-0.91	0.92	792.45	0.22	0.15
200	33.10	-0.79	0.39	35.78	-0.84	0.91	785.18	0.24	0.15
250	32.09	-0.78	0.41	35.64	-0.84	0.92	782.58	0.23	0.14
300	30.64	-0.78	0.40	33.68	-0.82	0.92	789.77	0.21	0.13
500	29.08	-0.78	0.34	41.96	-0.92	0.88	828.54	0.19	0.17
800	13.45	-0.65	0.14	26.54	-0.89	0.82	895.95	0.15	0.18
1000	1.96	-0.30	0.01	6.77	-0.67	0.53	944.42	0.05	0.05
1200	4.03	-12.40	0.02	0.08	-0.25	0.05	801.90	-0.03	0.03
In	25.46	-0.76	0.40	29.72	-0.83	0.91	***	***	***
Above	0.70	-0.15	0.01	1.01	-0.28	0.29	***	***	***